

Towards Speeding up Adversarial Training in Latent Spaces

Yaguan Qian, Qiqi Shao, Tengpeng Yao, Bin Wang, Shaoning Zeng, Zhaoquan Gu and Wassim Swaileh

Abstract—Adversarial training is widely considered as the most effective way to defend against adversarial examples. However, existing adversarial training methods consume unbearable time cost, since they need to generate adversarial examples in the input space, which accounts for the main part of total time-consuming. For speeding up the training process, we propose a novel adversarial training method that does not need to generate real adversarial examples. We notice that a clean example is closer to the decision boundary of the class with the second largest logit component than any other class besides its own class. Thus, by adding perturbations to logits to generate Endogenous Adversarial Examples(EAEs)—adversarial examples in the latent space, it can avoid calculating gradients to speed up the training process. We further gain a deep insight into the existence of EAEs by the theory of manifold. To guarantee the added perturbation is within the range of constraint, we use statistical distributions to select seed examples to craft EAEs. Extensive experiments are conducted on CIFAR-10 and ImageNet, and the results show that compare with state-of-the-art “Free” and “Fast” methods, our EAE adversarial training not only shortens the training time, but also enhances the robustness of the model. Moreover, the EAE adversarial training has little impact on the accuracy of clean examples than the existing methods.

Index Terms—Adversarial Training, Endogenous Adversarial Examples, Latent spaces.

I. INTRODUCTION

DEEP neural networks (DNNs) has been successfully applied in image recognition [1], speech recognition [2], natural language processing [3] and other fields. However, recent studies reveal that DNNs are seriously vulnerable to adversarial examples. An adversarial example is usually a natural image added by well-designed perturbations to mislead DNNs. Many methods are proposed to generate adversarial examples [4], [5], [6], [7], [8], [9]. Some recent works attempt to explore the possible reasons for explanation of adversarial examples [4], [5]. Nevertheless, it is still not fully understood due to the black-box characteristics of DNNs. At the same time, the corresponding defenses have also been extensively studied [5], [8], [10], [14], [15], in which adversarial training is considered to be the most effective defensive method at present [15].

Madry et. al [8] described adversarial training as a minimum and maximum saddle point optimization problem. The internal maximal problem is to find the strongest adversarial examples, while the external minimal problem is to obtain the least loss with the strongest adversarial examples. Therefore, the effect of adversarial training depends on the intensity of adversarial examples [8]. Existing research shows that the computational cost of adversarial training is very high [15]. Especially, the generation of adversarial examples accounts for the main

part of total time-consuming. For improving the efficiency of adversarial training, Shafahi et. al [15] proposed the “Free” method to reduce the number of gradient steps used for generating adversarial examples and Wong et. al [16] proposed the “Fast” method recently, just combining FGSM adversarial training with random initialization to achieve a defense as effective as PGD-based adversarial training. But these methods still rely on creating real adversarial examples in the input space by calculating the gradient of the loss. If the back-propagation for updating perturbations can be omitted, the performance of adversarial training can be further improved.

From this perspective, we propose an novel adversarial training method without generating real adversarial examples in the input space. The main idea is to add perturbations to the output of the penultimate layer, i.e., latent spaces termed in this paper. Contrast to an adversarial example in the input space, we denote an example added perturbations in the latent space as an *endogenous adversarial example* (EAE). Suppose $\mathcal{F}(x)$ is a pretrained model, and its logits $z = (z_1, z_2, \dots, z_C)$ of x , where C is the number of classes. Assume z_1 is the largest component and z_2 is the second largest component, then the class (*Class1*) corresponding to z_1 is consider as the predicted class with the maximum posterior rule. If this predicted result is correct, we think the class (*Class2*) responding to z_2 is more confused to the model than the remained classes to be misclassified to *Class1*. This can be confirmed from a geometric viewpoint as illustrated in Fig. 1. We believe the distance of the example x to the decision boundary between *Class1* and *Class2* is the closest. Therefore, we suggest that *Class2* is suitable for an adversarial targeted class in the latent space to ensure the smallest perturbation.

Unfortunately, the perturbation crafted in the latent space can not guarantee that its corresponding perturbation in the input space is within the range of constraint, such as L_2 or L_∞ bound, which is to avoid detection by human. We define the concepts of a *candidate seed example* and a *seed example* for the first time. A candidate seed example is accurately classified by the model for generating adversarial examples, but it is not surely crafted as an adversarial example. A seed example is certainly a candidate seed example, besides, it can be successfully crafted as an adversarial example by an specific attack method. Correspondingly, we term a candidate seed example added by perturbations as a *perturbed example* since it is not certainly an adversarial example. So if we can determine seed examples in advance, then the perturbation added to these seed examples in the latent space can satisfy the constraint in the input space.

To determine the seed examples is heuristic. We observe

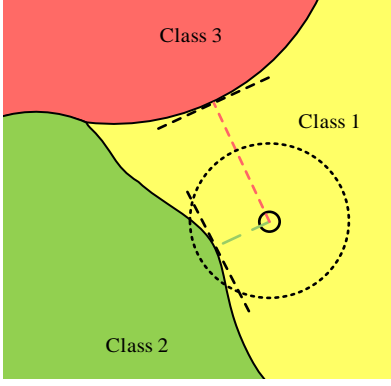


Fig. 1: Illustration of the decision boundary between Class1, Class2, and Class3. The circle with solid line represents the example x , and the circle with dotted line represents the perturbation bound.

that the difference of logit components between Class1 and Class2 of seed example and non-seed example has different distribution as shown in Fig. 2. Based on this observation, we propose a threshold mechanism to determine the seed examples. The threshold can be obtained by their distance distributions. If the difference of logit components between the Class1 and Class2 is less than the given threshold, then the example is selected to be crafted as an EAE for adversarial training. The advantage of this approach is that it can avoid calculating the gradient of loss with respect to examples and remarkably speed up the adversarial training.

Compared with the previous work, the contributions of our work are summarized as follows:

- 1) To the best of our knowledge, we are the first to propose EAE adversarial training without generating real adversarial examples. Our approach only needs to change logits of the penultimate layer to generate EAEs for training. Since no need to calculate the gradient of the loss with respect to the example, it remarkably improves the adversarial training speed.
- 2) We clearly define the concepts of a candidate seed example and a seed example for the first time, which emphasizes the fact that not any clean examples can be crafted to adversarial examples. With these concepts, we observe the difference of seed example and non-seed example in statistics, which helps to craft EAEs satisfying perturbation constraints. In addition, we gain an deep insight of the existence of EAEs with manifold theory.
- 3) Extensive experiments are conducted on CIFAR-10 and ImageNet. Experimental results show that the training time required for EAE adversarial training is about 1/3 of PGD adversarial training. And for clean examples, the model after EAE adversarial training does not significantly reduce its classification accuracy.

II. RELATED WORK

A. Adversarial Examples

Szegedy et al. [4] first discovered the existence of adversarial examples in DNNs, which can fool the DNN by adding tiny perturbations to clean examples. After then, Goodfellow et al. [5] proposed FGSM for quickly generating adversarial examples through one-step update along the gradient direction of the loss function to increase the loss. This method stems from their belief that the vulnerability of neural networks to adversarial examples is caused by its linear nature. Subsequently, Kurakin et al. [17] proposed BIM, which is an improvement to FGSM by converting a single-step attack into a multi-step attack with smaller steps to achieve a stronger adversarial example. In addition, Tramèr et al. [18] proposed RFGSM to enhance the FGSM attack effect by adding randomization steps. Similarly, Madry et al. [8] proposed PGD, strengthening iterative adversarial attacks by adding multiple random restart steps. This attack is considered the strongest first-order adversarial attack so far. The perturbations usually added by these methods are constrained by L_2 or L_∞ norm. However, according to Jacobian matrix, Papernot et al. [a3] defined an adversarial saliency map to limit the perturbation norm and only modify a few pixels of the clean example instead of perturbing the entire example to deceive classifier. Besides, Moosavi-Dezfooli et al. [9] found a general perturbation that not only makes a certain example misclassified, but also makes most examples obeying the same distribution in a dataset misclassified. Recently, Zhang et al. [19] proposed principal component adversarial examples on the assumption that the first k -principal component elements can form a data manifold. This kind of adversarial example does not depend on the model, and does not require to back-propagation to find the gradient of the loss to the example. All these methods craft adversarial examples in the input space, while our method manipulate logits in the latent space.

B. Adversarial Training

Goodfellow et al. [5] proposed FGSM adversarial training method, which use FGSM adversarial examples to train the model. However, FGSM adversarial training can not defend stronger adversarial examples. Madry proposed PGD adversarial training, which is considered as the best method so far. However, the cost of running a strong PGD adversary in the inner loop of training is very expensive. Some early work found that taking a larger step size but fewer iterations did not always significantly change the robustness of the network [20]. In order to reduce the computational overhead of the PGD defense, Shafahi et al. [15] focused on returning k -step PGD to a variant of its single-step FGSM predecessor, called “Free” adversarial training, which updated both model weights and input perturbation by using a single back-propagation. Zhang et al. [21] believed that when performing a multi-step PGD, redundant calculations can be cut down for additional acceleration during back-propagation when computing adversarial examples. Although these improvements are faster than standard adversarial training procedure, they are still much slower than traditional training methods. Therefore,

Wong et al. [16] proposed the “Fast” method, which used the previous minibatch’s perturbation or initialized a perturbation from uniformly random perturbation to add to the clean example, and used a step larger than the perturbation, plus the cyclic learning rate and technologies such as mixed-precision arithmetic enable “Fast” adversarial training to successfully resist PGD adversarial attacks.

However, these methods all rely on generating real adversarial examples, and calculate the gradient of loss to examples through back-propagation. Existing research shown [15] that the computational complexity of adversarial training was very high, and the generation of adversarial examples accounted for the main part of the total time. Therefore, if the step of generating adversarial examples can be omitted, it is possible to avoid calculating the gradient of the loss to example through back-propagation, which will greatly shorten the training time. Taking above view into consideration, we propose a novel training method that generates EAEs for training by changing the logit of the penultimate layer of the network, without the need to generate adversarial examples in the physical sense.

III. PROBLEM STATEMENT

A. Basic Definition

In this paper, we denote training data as $D = \{(\mathbf{x}_i, y_i)\}_{i=1}^N$, where $\mathbf{x}_i \in \mathbb{R}^D$, $y_i \in \{1, \dots, C\}$, and y_i is the class index of \mathbf{x}_i . Suppose $\mathcal{F}(\mathbf{x}; \boldsymbol{\theta})$ is a pre-trained neural network model with parameter $\boldsymbol{\theta}$, then $\mathcal{F}(\mathbf{x}; \boldsymbol{\theta}) = \mathcal{F}^{(N)}(\dots(\mathcal{F}^{(2)}(\mathcal{F}^{(1)}(\mathbf{x}))))$. Denote the output of the penultimate layer of the classifier \mathcal{F} , a vector of logits $\mathcal{F}^{(N-1)} = \mathbf{z} = (z_1, z_2, \dots, z_C)$, and the output of last layer as a probability vector $P = (p_1, p_2, \dots, p_C)$:

$$p_j = \text{Softmax}(\mathbf{z})_j = e^{z_j} / \sum_{k=1}^C e^{z_k}, j = 1, 2, \dots, C \quad (1)$$

where p_j is the confidence score that the example is discriminated as the j -th class. $\hat{y} = \arg \max_j \{p_j\}$ is the predicted class index of \mathbf{x} .

Szegedy et al. [4] first discovered adversarial examples in DNNs. After then, many techniques are proposed to generate adversarial examples with optimization methods [5], [6], [7], [8]. We formally defines adversarial examples as follows:

Definition 1. (Adversarial Examples) For a clean example $\mathbf{x} \in \mathcal{X}$, y is the ground-truth class index of \mathbf{x} . If a perturbation $\boldsymbol{\delta}$ with $\|\boldsymbol{\delta}\|_2 < \epsilon$ makes $\mathbf{x}' = \mathbf{x} + \boldsymbol{\delta}$ satisfies $\mathcal{F}(\mathbf{x}') \neq y$, then \mathbf{x}' is called an adversarial example.

Since the added perturbation $\boldsymbol{\delta}$ is constrained, and many methods use one-step approximation methods to reduce the computational cost, not all clean examples can be successfully crafted to the corresponding adversarial examples. Accordingly, we further divide the clean examples into *candidate seed examples* and *seed examples* in this paper.

Definition 2. (Candidate Seed Examples) Assume that G is an adversarial generation algorithm, any clean example $\mathbf{x} \in \mathcal{X}$ that can be accurately classified by \mathcal{F} is called a candidate seed example of G .

Definition 3. (Seed Examples) Suppose \mathbf{x} is a candidate seed example, y is the ground-truth label of \mathbf{x} , if $\mathcal{F}(G(\mathbf{x})) \neq y$, then \mathbf{x} is called a seed example of G on the model \mathcal{F} .

B. Endogenous Adversarial Examples

Traditional adversarial training needs to generate adversarial examples in the input space to train the classifier. However, generating the adversarial examples is more time-consuming [15]. Shafahi et. al [15] believed that the time complexity of adversarial training is mainly determined by the time to generate adversarial examples. Instead, our method is to perturb the logits of the penultimate layer of the network, which is called as endogenous adversarial examples for adversarial training. Training time can be effectively shortened since this endogenous adversarial example for adversarial training does not require generation of a real adversarial example in the input space. The formal definition is presented as follows:

Definition 4. (Endogenous Adversarial Examples) For a clean example $\mathbf{x} \in \mathcal{X}$, y is the ground-truth label of \mathbf{x} . The logits of \mathbf{x} passing the penultimate layer of the network is \mathbf{z} , and a perturbation Δ is added to logits, that is, $\mathbf{z}' = \mathbf{z} + \Delta$. If there is a corresponding \mathbf{x}' in the input space, which satisfies $\mathcal{F}(\mathbf{x}') = \text{Softmax}(\mathbf{z}') \neq y$, then \mathbf{x}' is referenced as a EAE.

C. Problem Setup

As we known, the so-called adversarial training is to utilize adversarial examples to train models for improving robustness. Here we obtain adversarial examples in the penultimate layer of DNNs, which is different from previous work crafting them in the input space. Thus we model the adversarial training as a two-level optimization problem as follows:

$$\begin{aligned} & \min_{\boldsymbol{\theta}} \mathcal{L}(\mathbf{z} + \Delta, \boldsymbol{\theta}) \\ & \text{s.t. } \arg \min_{\Delta} \|\Delta\|_2 \quad (2) \\ & z_y + \Delta_y < \max \{z_j + \Delta_j \mid 1 \leq j \leq C \wedge j \neq y\} \end{aligned}$$

where $\mathcal{L}(\cdot)$ is a loss function, \mathbf{z} is the penultimate layer output, and z_y is the largest element of logits corresponding to the class y . The up-level problem is to minimize loss function \mathcal{L} , while the low-level problem is to find the minimum perturbation Δ , as described in problem (2).

Instead of generating adversarial examples in the input space, we attempt to obtain a minimum perturbation Δ in the latent space instead of perturbation $\boldsymbol{\delta}$ in the input space. Assume that the true label y is consistent with the predicted label \hat{y} of the clean example \mathbf{x} , that is, $y = \hat{y}$. After passing the Softmax layer, the output of the EAE \mathbf{x}' is:

$$\begin{aligned} p'_j &= \text{Softmax}(\mathbf{z} + \Delta)_j \\ &= e^{z_j + \Delta_j} / \sum_{k=1}^C e^{z_k + \Delta_k}, \quad j = 1, 2, \dots, C \quad (3) \end{aligned}$$

where $y' = \arg \max_j \{p'_j\}$ is the predicted label of the EAE. From the definition of adversarial examples, we know that $y' \neq y \wedge y' \neq \hat{y}$, that is, $y \neq \arg \max_j \{p'_j\}$. Therefore, $\mathcal{F}(\mathbf{x}'; \boldsymbol{\theta}) \neq y$ means $\text{Softmax}(\mathbf{z} + \Delta)_y < \max \{\text{Softmax}(\mathbf{z} + \Delta)_j \mid 1 \leq j \leq C \wedge j \neq y\}$.

Since Softmax is a monotonically increasing function, the above inequality is equivalent to $z_y + \Delta_y < \max \{z_j + \Delta_j \mid 1 \leq j \leq C \wedge j \neq y\}$. Therefore, we express the process of generating EAEs as the following optimization problem:

$$\begin{aligned} & \min_{\Delta} \|\Delta\|_2 \\ \text{s.t. } & z_y + \Delta_y < \max \{z_j + \Delta_j \mid 1 \leq j \leq C \wedge j \neq y\} \end{aligned} \quad (4)$$

IV. IMPLEMENTATION

Given a set of clean examples, we first select seed examples for further generating EAEs. A threshold-based method using statistical distribution is introduced to address selecting seed examples. Then with these selected seed examples, we use optimization method to obtain EAEs. At the same time, the adversarial training are conducted with these EAEs.

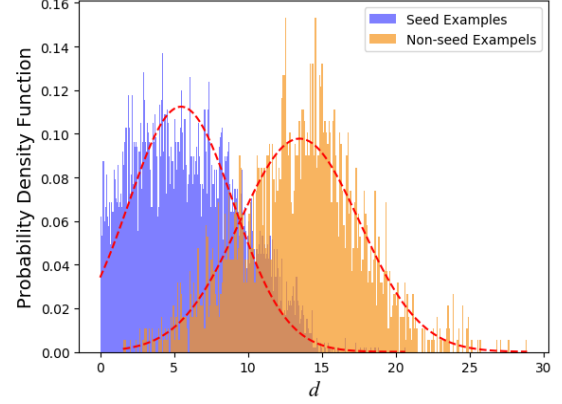
A. Selecting Seed Examples

Although we can find an minimum perturbation Δ in the latent space for each example by solving the problem (3), it cannot guarantee the corresponding perturbation δ in the input space to meet the constraint $\|\delta\|_2 < \epsilon$. Therefore, we need to give some constraints to Δ , however, it is nontrivial since the relationship between δ and Δ is not linear. In this paper, we propose a method based on statistical distribution to observe the seed examples.

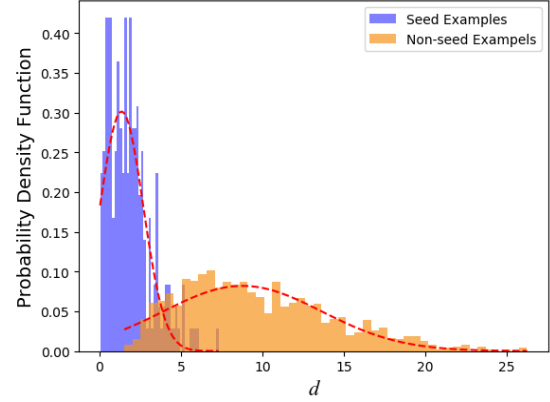
Remind that every clean example accurately classified by the model has a chance to be crafted as adversarial examples in theory, which are referred as *candidate seed examples* in this paper. In fact, under the constraint $\|\delta\|_2 < \epsilon$, only these examples nearby the decision boundary can finally be crafted as adversarial examples, which are referred as *seed examples*. If we select all possible seed examples, then we can craft *endogenous adversarial examples* that $\mathcal{F}(\mathbf{x} + \delta) = \text{Softmax}(\mathbf{z} + \Delta)$, s.t. $\|\delta\|_2 < \epsilon$.

Let $d = z_y - z_s$ denote the difference between the largest element and the second largest element in logits of the example. For convenient description, we refer this difference as LD (Logits Difference). Our experiment shows that for seed examples, LD is small, while for non-seed examples, LD is large. In addition, Fig. 1 shows that LDs of both seed examples and non-seed examples follows the Gaussian distribution. Thus, we introduce a threshold γ to select the seed examples. If a clean example satisfies $d < \gamma$, we believe it may be a seed example with a large confidence. With this simple rule, we can find most of the seed examples to reduce more time for further generating adversarial examples.

We determine the value of γ by empirical value. First, some clean examples that correctly classified by the model are remained as a set of candidate seed example $\tilde{D} = \{(\mathbf{x}_i, y_i)\}_{i=1}^M$, where $\tilde{D} \subset D$ and $|\tilde{D}| \ll |D|$. If the clean example $\mathbf{x} \in D$ can be perturbed successfully by an adversarial generation algorithm G , then \mathbf{x} is remained to the set of seed examples D^+ , otherwise it is remained to the set of non-seed examples D^- . Obviously, $D^+ \cup D^- = \tilde{D}$. Then, we can obtain the difference between the largest element and the second largest



(a) CIFAR-10



(b) ImageNet

Fig. 2: LD distribution of seed examples and non-seed examples: (a) on CIFAR-10, when FGSM is carried out on F_1 and $\epsilon = 0.05$, LD distribution of seed examples and non-seed examples; (b) on ImageNet, when FGSM is carried out on F_3 and $\epsilon = 0.002$, LD distribution of seed examples and non-seed examples.

element in logits of the example in D^+ and D^- respectively as shown in Fig. 2. We use the mean of LD denoted by \bar{d} , which is called as MLD in this paper, in D^+ as the threshold γ . Since our EAE adversarial training does not strictly require that all seed examples must generate EAEs, the threshold determined by this statistical method is more reliable.

B. Generating EAEs

After selecting the seed example, we need to add perturbation to it to generate EAE by solving problem (3). Take a deep insight into problem (3), we observed that obtaining the minimum perturbation with the constraint only need to find the second largest value in $z_j (1 \leq j \leq y)$ corresponding to the second largest likelihood class. Let z_s denote the second largest value: $z_s = \max \{z_j \mid 1 \leq j \leq C \wedge j \neq y\}$, such that $z_y + \Delta_y < z_s + \Delta_s$, where Δ_y is the perturbation added on z_y and Δ_s is the perturbation added on z_s . Obviously, when

$\Delta_j = 0$ where $1 \leq j \leq C \wedge (j \neq y \wedge j \neq s)$, then $\|\Delta\|_2$ reaches the minimum and $\|\Delta\|_2 = \sqrt{\Delta_y^2 + \Delta_s^2}$. Since $\min \Delta_y^2 + \Delta_s^2$ is equivalent to $\min \sqrt{\Delta_y^2 + \Delta_s^2}$, the optimization problem (3) can be expressed as:

$$\begin{aligned} & \arg \min_{\Delta_y, \Delta_s} \Delta_y^2 + \Delta_s^2 \\ \text{s.t. } & z_y + \Delta_y < z_s + \Delta_s \end{aligned} \quad (5)$$

Since the constraint $z_y + \Delta_y < z_s + \Delta_s$ in problem (5) cannot determine the boundary of feasible regions, we further relax the constraints as $z_y + \Delta_y \leq z_s + \Delta_s$. Although this relax cannot guarantee that the example added with the perturbation Δ can become an EAE, we can ensure $z_y + \Delta_y = z_s + \Delta_s$, i.e., the confidence of the Class1 and Class2 are equal. This case indicates the perturbed example is moved to the decision boundary between the first-likelihood and the second-likelihood class. Accordingly, the perturbed example has a 50% probability to be classified as one of the top-2 classes. Our adversarial training does not strictly require that each clean example become an EAE.

After relaxing the constraint, the problem can be rewritten as follows:

$$\begin{aligned} & \arg \min_{\Delta_y, \Delta_s} \Delta_y^2 + \Delta_s^2 \\ \text{s.t. } & z_y + \Delta_y \leq z_s + \Delta_s \end{aligned} \quad (6)$$

We use Lagrange multiplier method to solve this problem. The Lagrangian function can be written as follows:

$$L(\Delta_y, \Delta_s, \lambda) = \Delta_y^2 + \Delta_s^2 + \lambda(\Delta_y - \Delta_s + z_y - z_s) \quad (7)$$

Its optimality conditions are:

$$\begin{cases} \frac{\partial L}{\partial \Delta_y} = 2\Delta_y + \lambda = 0 \\ \frac{\partial L}{\partial \Delta_s} = 2\Delta_s - \lambda = 0 \\ \lambda(\Delta_y - \Delta_s + z_y - z_s) = 0 \\ \lambda \geq 0 \end{cases} \quad (8)$$

So when $\lambda = 0$, then $\Delta_y = 0$, $\Delta_s = 0$; when $\Delta_y - \Delta_s + z_y - z_s = 0$, then $\Delta_y = -(z_y - z_s)/2$, $\Delta_s = (z_y - z_s)/2$, $\lambda = z_y - z_s$. Obviously, the former does not meet the solution of problem (6). In summary, the approximate optimal solution of problem (4) is $\Delta^* = (\Delta_1, \dots, \Delta_j, \dots, \Delta_C)$,

$$\Delta^* = \begin{cases} -(z_y - z_s)/2, & j = y \\ (z_y - z_s)/2, & j = s \\ 0, & j \neq y \wedge j \neq s \end{cases} \quad (9)$$

C. Adversarial Training with EAEs

We utilize SGD to train the DNN and divide the training dataset D into K minibatch. Suppose the initial parameters of the DNN are θ_0 , the algorithm will generate all of EAEs in the first minibatch. With these EAEs, the gradient of lost function is obtained and then update the model parameters by back-propagation. After the first minibatch update, we have the new model parameters θ_1 . With the new model parameters, the algorithm starts the next iteration based on the second minibatch. This iterative update will continue until K minibatch are processed, which we say an epoch is finished. For achieve a perfect effect, multiple epochs are generally conducted.

Algorithm 1 Adversarial training with EAEs

Input: $D = \{(x_i, y_i)\}_{i=1}^N$; T is the number of epochs; K is the number of minibatch; M is the size of minibatch; γ is the threshold

Output: θ

```

1: for  $t = 1, \dots, T$  do
2:   for  $i = 1, \dots, K$  do
3:     for  $j = 1, \dots, M$  do
4:        $z_j \leftarrow F^{(N-1)}(\dots(F^{(2)}(F^{(1)}(x_j))))$ 
5:        $z_y \leftarrow \max(z_j)$ 
6:        $z_s \leftarrow \sec(z_j)$ 
7:       if  $z_y - z_s < \gamma$  then
8:          $z_j \leftarrow z_j + \Delta_j$ 
9:       end if
10:    end for
11:     $\mathcal{L} \leftarrow \frac{1}{M} \sum_{i=1}^M \mathcal{L}(z_j, y_j)$ 
12:     $\theta \leftarrow \theta - \eta \cdot \nabla_{\theta} \mathcal{L}$ 
13:  end for
14: end for
```

V. INTERPRETATION OF EAEs

In this section, we make an attempt to interpret the existence of EAEs through the theory of manifold. We first introduce the notation and basic definitions of the manifold for the ease of better understanding of our further analysis.

Definition 5. (Manifolds) A d -dimensional manifold M is set that is locally homeomorphic with \mathbb{R}^d . That is, for each $x \in M$, there is an open neighborhood around x , N_x , and a homeomorphism $f : N_x \rightarrow \mathbb{R}^d$. These neighborhoods are referred to as coordinate patches, and the map is referred to a coordinate chart. The image of the coordinate charts is referred to as the parameter space [22].

According to manifold hypothesis, real-world data presented in high-dimensional spaces are expected to concentrate in the vicinity of a manifold M of much lower dimensionality \mathbb{R}^d embedded in \mathbb{R}^D ($D > d$). In other words, a d -dimensional manifold M passes through the D -dimensional data space.

Let M be the d dimensional manifold. This manifold M is an embedded submanifold of \mathbb{R}^D . Let $P : \mathbb{R}^D \rightarrow M$ be the projection operator onto M , i.e.,

$$P(v) = \arg \min_{w \in M} \|w - v\|_2$$

Given a point $x \in \mathbb{R}^D$, suppose that there exists a unique projection point x_* of x onto M , i.e.,

$$x_* = P(x).$$

By the continuity of projection operator, there exists a positive constant $\delta_1 > 0$ such that for any $x' \in B(x, \delta_1)$, the projection $P(x')$ is well-defined. Since $B(x, \delta_1)$ is compact, there exists a positive constant $c_0 > 0$ such that

$$\begin{aligned} \text{dist}(P(x'), x_*) &= \text{dist}(P(x'), P(x)) \leq c_0 \|x' - x\|_2 \leq c_0 \delta_1, \\ x' &\in B(x, \delta_1) \end{aligned} \quad (10)$$

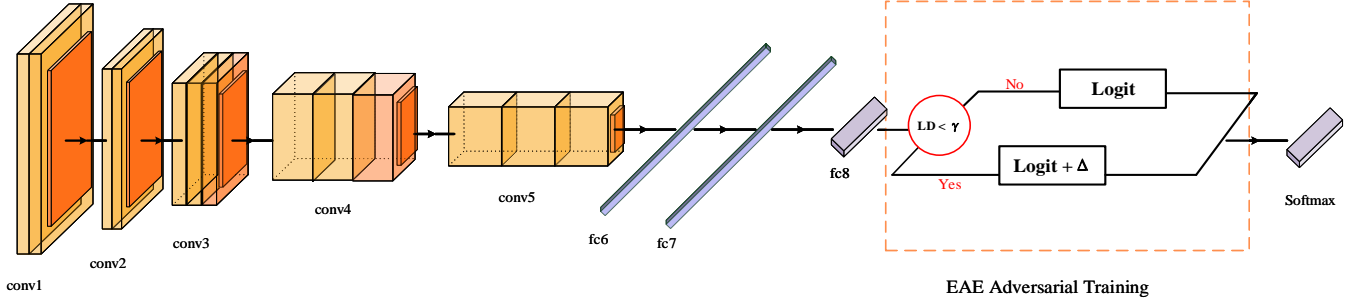


Fig. 3: Schematic diagram of EAE adversarial training method.

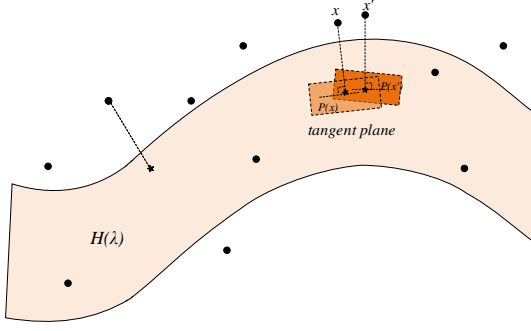


Fig. 4: Examples x and x' in D -dimensional space are projected onto the d -dimensional manifold via P .

By the above inequality, we have

$$P(B(x, \delta_1)) \subset B(x_*, c_0 \delta_1) \quad (11)$$

Let U be an open bounded subset of \mathbb{R}^d and $H : U \subset \mathbb{R}^d \rightarrow M$ be a local parametrization of M such that

$$H(\lambda) = x_*, \quad B(x_*, c_0 \delta_1) \subset H(U)$$

Since H is diffeomorphism defined from $U \subset \mathbb{R}^d$ to $H(U) \subset M$, the set $H^{-1}(B(x_*, c_0 \delta_1))$ is a compact neighborhood of λ .

Since H is an embedded submanifold, the differential $DH(\tilde{\lambda}) : \mathbb{R}^d \rightarrow T_{H(\tilde{\lambda})}M$ is injective for any point $\tilde{\lambda} \in U$. By the compactness of $H^{-1}(B(x_*, c_0 \delta_1))$, there exist two positive constant $c_1 < c_2$ such that

$$c_1 \|\Delta \tilde{\lambda}\|_2 \leq \|DH(\tilde{\lambda})[\Delta \tilde{\lambda}]\|_2 \leq c_2 \|\Delta \tilde{\lambda}\|_2, \quad \forall \tilde{\lambda} \in H^{-1}(B(x_*, c_0 \delta_1)), \Delta \tilde{\lambda} \in \mathbb{R}^d \quad (12)$$

Given a point $x' \in B(x, \delta_1)$, denote $x'_* = P(x')$. Since $x'_* \in B(x_*, c_0 \delta_1)$, there exists a unique point $\lambda' \in H^{-1}(B(x_*, c_0 \delta_1))$ such that $x'_* = H(\lambda')$ [23]. Thus we have

$$\begin{aligned} \gamma_1 \int_0^1 \|DH(\lambda + t(\lambda' - \lambda))[\lambda' - \lambda]\|_2 dt &\leq \text{dist}(x'_*, x_*) \\ &\leq \int_0^1 \|DH(\lambda + t(\lambda' - \lambda))[\lambda' - \lambda]\|_2 dt \end{aligned} \quad (13)$$

where $0 < \gamma_1 \leq \frac{\text{dist}(x'_*, x_*)}{\int_0^1 \|DH(\lambda + t(\lambda' - \lambda))[\lambda' - \lambda]\|_2 dt}$.

By (13) and (14), we have

$$c_1 \gamma_1 \|\lambda' - \lambda\|_2 \leq \text{dist}(x'_*, x_*) \leq c_2 \|\lambda' - \lambda\|_2 \quad (14)$$

According to (11) and (15), we can obtain

$$\begin{aligned} \|\lambda' - \lambda\|_2 &\leq \frac{1}{c_1 \gamma_1} \text{dist}(x'_*, x_*) = \frac{1}{c_1 \gamma_1} \text{dist}(P(x'), P(x)) \\ &\leq \frac{c_0}{c_1 \gamma_1} \|x' - x\|_2 \end{aligned} \quad (15)$$

Thus small perturbation of x induces small perturbation of λ . Fig. 4 illustrates the projection procedure.

VI. EXPERIMENTS

A. Experimental Setup

Datasets: Two popular benchmark datasets CIFAR-10 and ImageNet are used to evaluate our EAE adversarial training algorithm. CIFAR-10 has 60,000 color images with the size of 32×32 and 10 categories. In each category, there are 6,000 images included. We hold 50,000 images as a training set, and the rest 10,000 images as a test set. For ImageNet, we only randomly extract examples with 30 categories and each category includes 1,350 images with the size of 224×224 , which is termed as ImageNet-30 in this paper. We hold 39,000 images as a training set, and 1,500 images as a test set.

Our experiment is based on fully black-box attacks, that is, the network for generating perturbed examples (may not be adversarial examples attacked successfully) is fully different from the target network for adversarial training. Therefore, we choose the following deep neural network architecture for our experiments.

Models: For CIFAR-10, we first train a ResNet-18 model F_1 on CIFAR-10 training set with 15 epochs to select seed examples. Then we train the VGG-16 model F_2 on CIFAR-10 training set with 15 epochs to generate perturbed examples as a test set for our method. Since our experiments are conducted in full black-box settings, we conduct adversarial training on ResNet-18 that is different from the model VGG-16 used for generating perturbed examples.

For ImageNet, we use the pre-training models AlexNet and ResNet-18 provided by Pytorch as initial models for further training, and reduce their output classes to 30. We first train a AlexNet model F_3 on ImageNet with 4 epochs for selecting seed examples. Then we train the ResNet-18 model F_4 with 4 epochs to generate perturbed examples as a test set for our

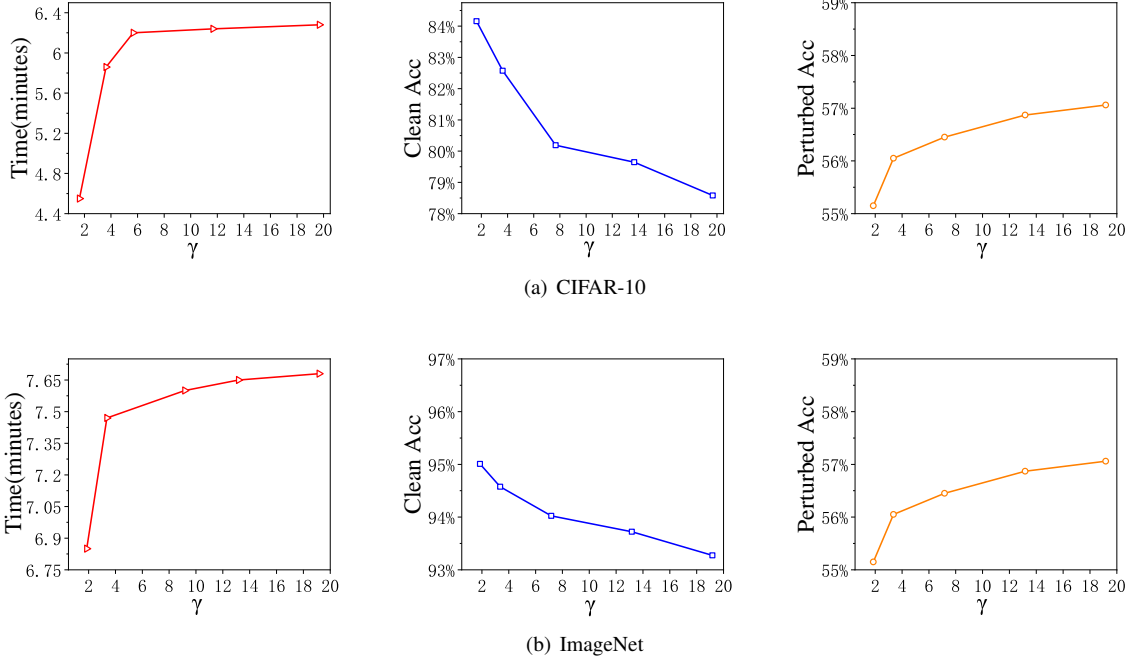


Fig. 5: The impact of the threshold γ on time, clean accuracy, and perturbed accuracy of the model after EAE adversarial training: (a) the perturbed examples used for test are from CIFAR-10. They are generated by FGSM on the model F_1 with the perturbation bound $\epsilon = 0.05$; (b) the perturbed examples used for test are from ImageNet. They are also generated by FGSM on the model F_3 with the perturbation bound $\epsilon = 0.007$.

TABLE I: The number of seed examples and non-seed examples and the corresponding MLD after adding different perturbations to CIFAR-10 testset

ϵ	Num(Seed)	MLD(Seed)	Num(Non-Seed)	MLD(Non-Seed)
0.01	2,299	3.63	6,883	11.85
0.02	3,949	4.68	5,233	12.36
0.03	5,051	5.26	4,131	12.82
0.04	5,839	5.66	3,343	13.21
0.05	6,441	5.98	2,741	13.50

TABLE II: The number of seed examples and non-seed examples and the corresponding MLD after adding different perturbations to ImageNet testset

ϵ	Num(Seed)	MLD(Seed)	Num(Non-Seed)	MLD(Non-Seed)
0.002	241	1.86	1,081	9.77
0.004	447	3.36	875	10.87
0.006	642	4.47	680	11.97
0.008	779	5.17	543	12.87

method. Considering black-box settings, we choose the model AlexNet that is different from the model ResNet-18 used for generating perturbed examples to conduct adversarial training

Our experiment is implemented by PyTorch1.4 with 4 2080ti GPUs and the operating system is Ubuntu16.04.6 LTS. A cyclic learning rate [24] is used to improve convergence and reduce the amount of tuning required when training networks. The cyclic learning rate can greatly reduce the number of epochs[25] required for deep neural network training.

B. Validation of Threshold Mechanism

We first select seed examples on CIFAR-10 and ImageNet. As described in Sec. IV-A, an appropriate threshold plays a critical role. On CIFAR-10, we perform FGSM on the model F_1 with perturbation bound $\epsilon = 0.01$ to construct the seed example set D^+ and non-seed example set D^- respectively. We obtain the MLD $\bar{d}_1 = 3.63$ on D^+ and $\bar{d}_2 = 11.85$ on D^- . Obviously, \bar{d}_1 is quite different to \bar{d}_2 . For further explore the impact of ϵ , we change it with the values 0.01, 0.02, 0.03, 0.04, and 0.05 and repeat the above process. MLDs with different ϵ are presented in Table 1. It shows that although the MLD of both the seed example and the non-seed example raises with the increase of ϵ , the difference between them still maintains large (about 7.54~8.22), which indicates the feasibility of our threshold mechanism.

On ImageNet, we similarly perform FGSM on model F_3 with $\epsilon = 0.002, 0.004, 0.006$, and 0.008 , and obtain D^+ and D^- respectively. The results are showed in Table 2. Similar to Table 1, it also demonstrates that the LD of the seed examples is smaller that of non-seed examples by 6.76~7.91.

C. Impact of Threshold

As mentioned in Sec. VI-B, the threshold γ is a function of the perturbation bound ϵ , thus a different ϵ will lead to a different γ . Therefore, we need to determine a reasonable γ by discussing its influence on adversarial training with EAEs. In this section, we discuss the relationship of γ with (1) the adversarial training time, (2) the accuracy of clean examples

(*Clean Acc*), and (3) the accuracy of perturbed examples (*Perturbd Acc*).

Adversarial training time: Fig. 5 shows the adversarial training time with respect to the threshold. We can observe that with the raise of threshold, the adversarial training time presents an increasing trend. For CIFAR-10, the training time increases dramatically before $\gamma = 5.98$; while after $\gamma = 6$, it almost not change. The reason is when $\gamma = 6$, almost total examples have been crafted as EAEs, thus increasing the threshold will not increase the training time accordingly. Similarly, for ImageNet, when $\gamma > 15$, the training time tends to be stable.

Accuracy of clean examples: Fig. 5 shows the accuracy of the model after adversarial training with different thresholds on clean examples. For both CIFAR-10 and ImageNet, the accuracy on clean examples decreases accordingly with the raise of the threshold γ . Especially on CIFAR-10, the difference between the maximum and minimum prediction accuracy is about 5.9%, which indicates that larger γ will severely degrade the accuracy of clean examples.

Accuracy of perturbed examples: Fig. 5 shows the accuracy of the model after adversarial training with different thresholds on perturbed examples. For CIFAR-10, the accuracy improves to some extent with the increasing threshold on perturbed examples, however this improvement is not salient, which does not exceed 1.6%. For ImageNet, the accuracy of perturbed examples is only improved by 2% even the threshold γ increasing from 1.86 to 19.17, which indicates that larger threshold does not improve the effect of adversarial training.

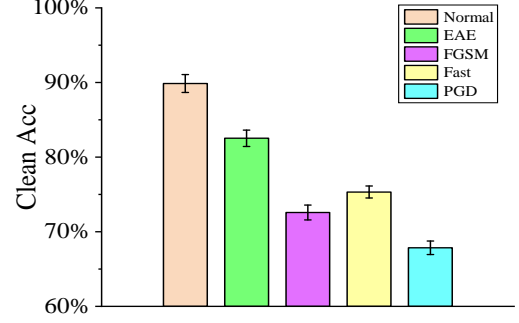
Based on the above analysis, we need to make a trade-off between the training time and accuracy. A smaller threshold can speed up the adversarial training with EAEs, at the same time, it can achieve a sound accuracy on clean examples compared to a little loss of robust. As a thumb-rule, we suggest $\gamma \in [2, 4]$ is proper for any data sets.

D. Effectiveness of Adversarial Training

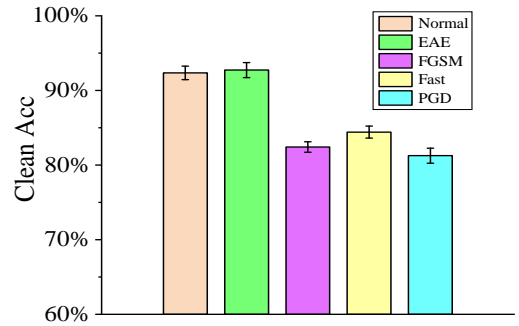
In this section, we compare our EAE adversarial training with the following three types of adversarial training, FGSM adversarial training, Fast adversarial training, and PGD adversarial training.

For CIFAR-10, we choose ResNet-18 as a classifier. Four ResNet-18 classifiers will be obtained by four types of adversarial training with $epoch = 4$, the minimum cyclic learning rate $clr_{min} = 0$, and the maximum cyclic learning rate $clr_{max} = 0.2$. Especially, for our EAE adversarial training, the threshold $\gamma = 3.63$; for FGSM adversarial training, the perturbation bound $\epsilon = 16/255$; for Fast adversarial training, $\epsilon = 16/255$ and the step size $\alpha = 20/255$; and for PGD adversarial training, $\epsilon = 16/255$, $\alpha = 8/255$, and the number of iteration $K = 7$. In addition, we also train a ResNet-18 classifier with clean examples as a benchmark. The test set consists of perturbed examples generated by the model F_2 (VGG-16).

For ImageNet, we choose AlexNet as a classifier. Four AlexNet classifiers will be obtained by four types of adversarial training with $epoch = 4$, $clr_{min} = 0$, and $clr_{max} = 0.02$.



(a) CIFAR-10



(b) ImageNet

Fig. 6: The accuracy of a normal trained model compared with adversarial trained models on clean examples: (a) 9,182 clean examples from CIFAR-10, all of which can be classified correctly by F_2 ; (b) 1,322 clean examples from ImageNet, all of which can be classified correctly by F_4 .

Especially, for our EAE adversarial training, the threshold $\gamma = 2.0$; for FGSM adversarial training, $\epsilon = 0.01$; for Fast adversarial Training, $\epsilon = 0.01$, $\alpha = 3/255$; and for PGD adversarial training, $\epsilon = 0.01$, $\alpha = 1/255$, $K = 4$. In addition, we also train a ResNet-18 classifier with clean examples as a benchmark. The test set consists of perturbed examples generated by the model F_4 (ResNet-18).

The accuracy of clean examples of the classifier after adversarial training: It can be seen from Fig. 6 that compared with normal training, adversarial training in general will reduce the classification accuracy on clean examples. However, our EAE adversarial training does not decrease the accuracy of the clean examples on ImageNet, while other three types of adversarial training decrease significantly. On CIFAR-10 the accuracy decrease. Nevertheless, the accuracy of our EAE adversarial training is higher than others by 7.21%~14.68%. On ImageNet, the accuracy of our EAE adversarial training is higher than others by 8.31%~11.47%.

Why does our EAE adversarial training not seriously reduce the accuracy of clean examples? Since our method generating EAEs is to move the example to the decision boundary of the

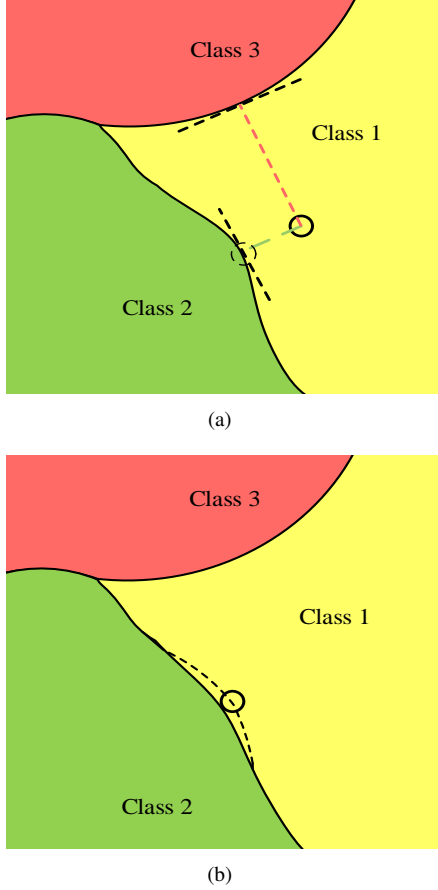


Fig. 7: Change of decision boundaries. (a) Generate an EAE; (b) Fine-tune decision boundary after EAE adversarial training.

first and second classes at a geometric point of view, and they will still be correctly classified with a probability of 50%. Thus, use these perturbed examples to train the model, the parameters are fine-tuned and the decision boundary merely change little as shown in Fig. 7. So it has less influence on the classification accuracy of the clean examples. Remind other adversarial training methods, the adversarial examples they used such as PGD may cross and go far from the decision boundary, which lead the adversarial training to adjust the decision boundary with large magnitude. As a result, some clean examples are misclassified by this new decision boundary.

The accuracy of perturbed examples of the classifier after adversarial training: Fig. 8 present the accuracy of perturbed examples on the models with normal training or adversarial training with respect to ϵ . Remind that F_2 and F_4 are used to generate perturbed examples respectively on CIFAR-10 and ImageNet to evaluate the robustness of the classifier. We observed that the proportion of adversarial examples increases with the perturbation bound ϵ or the number of iterations, which is consistent with our intuition. In essence, the accuracy of F_2 or F_4 represents the proportion of adversarial examples in the perturbed examples, and the lower accuracy of F_2 or F_4 indicates the more adversarial examples contained.

TABLE III: The training time required for four types of adversarial trainings

	EAE	FGSM	Fast	PGD
CIFAR-10	2.86 min	7.63 min	7.73 min	17.37 min
ImageNet	4.25 hrs	12.54 hrs	15.59 hrs	53.45 hrs

We observed that on CIFAR-10, increasing ϵ make the accuracy decrease 2% ~ 15% for our EAE adversarial training compared with the other three adversarial training methods that are not obviously affected by ϵ . However, compared with the normal training, our EAE adversarial training can improve the accuracy by 11%~39%, which indicates it can indeed enhance the robustness of the model.

On ImageNet, the robustness of the model after EAE adversarial training is better than other adversarial training methods, and its accuracy is about 7%~10% higher than other methods. We also found that the robustness of the model after FGSM, Fast, and PGD adversarial training is even worse than that of normal training. Especially, PGD adversarial training is the worst.

Why can our EAE adversarial training can improve the robustness of the model? As shown in Fig. 1, given a perturbation bound, if a clean example intend to be crafted as an adversarial example, our method chooses the class with the second large logit component as its adversarial target class. In other words, it moves the clean example towards the closest decision boundary. In fact, we change the maximum and the second largest value in logits during the adversarial training, and then update the parameters through back-propagation. The decision boundary adjusted by this method can defend against a large number of adversarial examples of which corresponding clean examples can easily generate adversarial examples into the second class.

E. Time Cost of Adversarial Training

In Table III, we can clearly see that our EAE adversarial training is fast than other methods, since it does not need to generate real adversarial examples, and hence does not need to calculate the gradient of the loss with respect to the example. Compared with FGSM adversarial training on CIFAR-10 and ImageNet, our method is faster by 4.77 minutes and 8.29 hrs, respectively. Compared with the slowest PGD adversarial training method, our EAE adversarial training reduces the time by about 4/5.

VII. CONCLUSION

In this paper, we propose a novel EAE adversarial training method without generating real adversarial examples to participate in training. The experiment results show that our method can speed the adversarial training process, which outperforms state-of-the-art “Fast” method. Especially, our EAE adversarial training has little impact on the accuracy of clean examples, which is a challenge in previous methods.

REFERENCES

- [1] Meiyin Wu and Li Chen, “Image recognition based on deep learning,” in *2015 Chinese Automation Congress(CAC)*, IEEE, 2015, pp. 542-546.

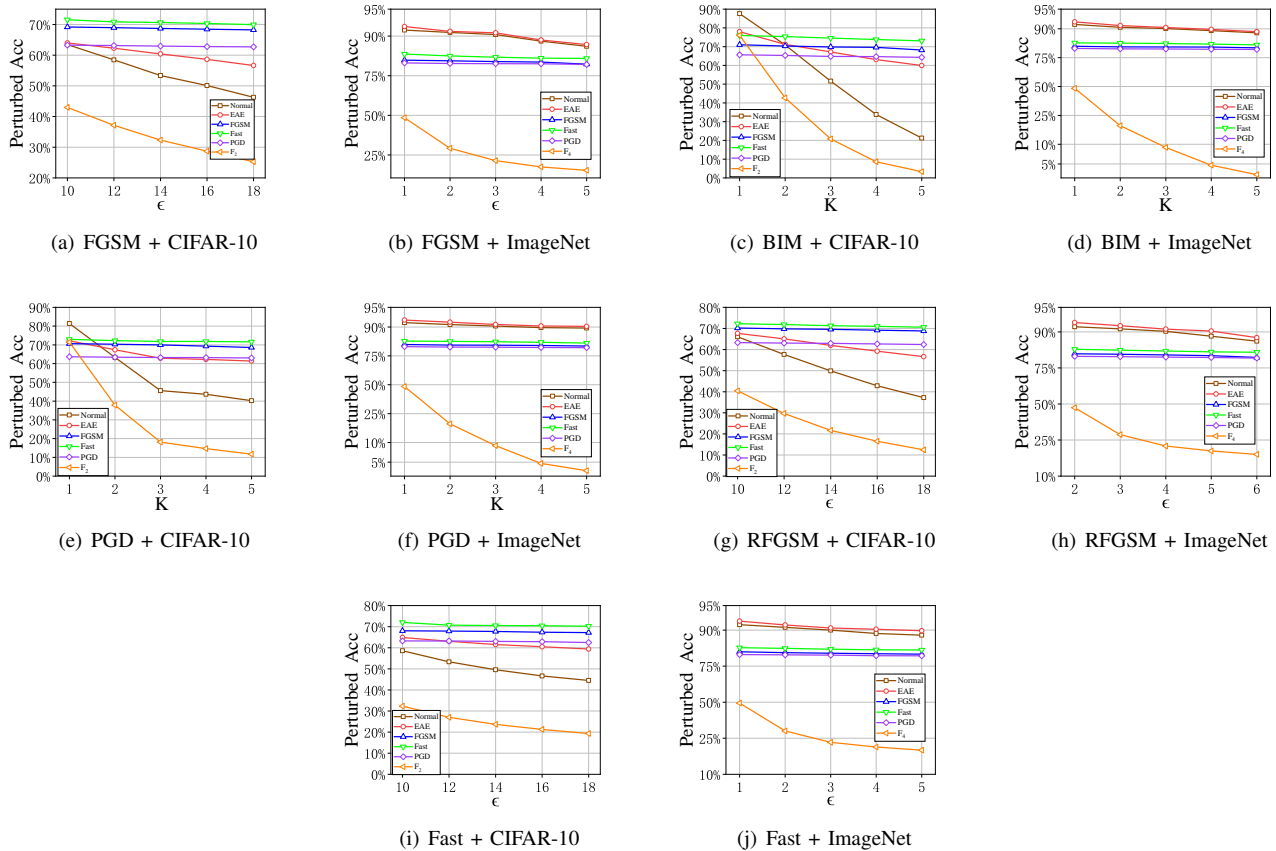


Fig. 8: The accuracy of the models with Normal, EAE, FGSM, Fast, and PGD adversarial training with respect to the perturbation bound ϵ and the number of iteration K . The test perturbed examples generated by (a) FGSM on CIFAR-10 with the perturbation bound $\epsilon/255$, (b) FGSM on ImageNet with $\epsilon/255$, (c) BIM on CIFAR-10 with $\epsilon = 12/255$, step size $\alpha = 4/255$, and $K = 1, \dots, 5$, (d) BIM on ImageNet with $\epsilon = 2/255$, $\alpha = 1/255$, and $K = 1, \dots, 5$, (e) PGD on CIFAR-10 with $\epsilon = 12/255$, $\alpha = 4/255$, and $K = 1, \dots, 5$, (f) PGD on ImageNet with $\epsilon = 4/255$, $\alpha = 1/255$, and $K = 1, \dots, 5$. (g) RFGSM on CIFAR-10 $\epsilon/255$, $\alpha = 4/255$, $K = 1$, (h) RFGSM on ImageNet with $\epsilon/255$, $\alpha = 1/255$, and $K = 1$, (i) Fast on CIFAR-10 $\epsilon/255$, and $\alpha = 20/255$, (j) Fast on ImageNet with $\epsilon/255$, and $\alpha = 6/255$.

- [2] Kuniaki Noda, Yuki Yamaguchi, Kazuhiro Nakadai, Hiroshi G. Okuno, and Tetsuya Ogata, "Audio-visual speech recognition using deep learning," in *Applied Intelligence*, 2015.
- [3] Ronan Collobert, and Jason Weston, "A unified architecture for natural language processing: Deep neural networks with multitask learning," in *Proceedings of the 25th international conference on Machine learning (ICML)*, 2008, pp. 160-167.
- [4] Christian Szegedy, Wojciech Zaremba, Ilya Sutskever, Joan Bruna, Dumitru Erhan, Ian Goodfellow, and Rob Fergus, "Intriguing properties of neural networks," 2013, arXiv:1312.6199. [Online] Available: <http://arxiv.org/abs/1312.6199>.
- [5] Ian J. Goodfellow, Jonathon Shlens, and Christian Szegedy, "Explaining and harnessing adversarial examples," in *International Conference on Learning Representations (ICLR)*, 2015.
- [6] Nicolas Papernot, Patrick McDaniel, Somesh Jha, Matt Fredrikson, Z. Berkay Celik, and Ananthram Swami, "The limitations of deep learning in adversarial settings," in *2016 IEEE European Symposium on Security and Privacy (EuroS&P)*, IEEE, 2016, pp. 372-387.
- [7] Seyed-Mohsen Moosavi-Dezfooli, Alhussein Fawzi, and Pascal Frossard, "Deep-fool: a simple and accurate method to fool deep neural networks," in *2016 IEEE Conference on Computer Vision and Pattern Recognition (CVPR)*, 2016, pp. 2574-2582.
- [8] Aleksander Madry, Aleksandar Makelov, Ludwig Schmidt, Dimitris Tsipras, and Adrian Vladu, "Towards deep learning models resistant to adversarial attacks," in *International Conference on Learning Representations (ICLR)*, 2018.
- [9] Seyed-Mohsen Moosavi-Dezfooli, Alhussein Fawzi, Omar Fawzi, and Pascal Frossard, "Universal adversarial perturbations," in *2017 IEEE Conference on Computer Vision and Pattern Recognition (CVPR)*, 2017, pp. 86-94.
- [10] Nicolas Papernot, Patrick McDaniel, Xi Wu, Somesh Jha, and Ananthram Swami, "Distillation as a defense to adversarial perturbations against deep neural networks," in *IEEE Symposium on Security and Privacy (SP)*, 2016, pp. 582-597.
- [11] Shixiang Gu., and Luca Rigazio, "Towards deep neural network architectures robust to adversarial examples," 2014, arXiv:1412.5068. [Online] Available: <https://arxiv.org/abs/1412.5068>.
- [12] Osbert Bastani, Yani Ioannou, Leonidas Lampropoulos, Dimitrios Vytiniotis, Aditya V. Nori, and Antonio Criminisi, "Measuring neural net robustness with constraints," in *Neural Information Processing Systems (NIPS), The Thirtieth Annual Conference on 2016*, 2016.
- [13] Ruitong Huang, Bing Xu, Dale Schuurmans, and Csaba Szepesvári, "Learning with a strong adversary," 2015, arXiv:1511.03034. [Online] Available: <https://arxiv.org/abs/1511.03034>.
- [14] Uri Shaham, Yutaro Yamada, and Sahand Negahban, "Understanding adversarial training: Increasing local stability of neural nets through robust optimization," in *Neurocomputing*, 2018, pp. 195-204.
- [15] Ali Shafahi, Mahyar Najibi, Amin Ghiasi, Zheng Xu, John Dickerson, Christoph Studer, Larry S. Davis, Gavin Taylor, and Tom Goldstein, "Adversarial Training for Free!" in *Advances in Neural Information Processing Systems (NIPS)*, 2019, pp. 3353-3364.
- [16] Eric Wong, Leslie Rice, and J. Zico Kolter, "Fast is better than free: revisiting adversarial training," in *International Conference on Learning Representations (ICLR)*, 2020.

- [17] Alexey Kurakin, Ian J. Goodfellow and Samy Bengio, "Adversarial examples in the physical world," in *International Conference on Learning Representations(ICLR)*, 2017.
- [18] Florian Tramèr, Alexey Kurakin, Nicolas Papernot*, Ian Goodfellow, Dan Boneh and Patrick McDaniel, "Ensemble adversarial training: Attacks and defenses," in *International Conference on Learning Representations(ICLR)*, 2018.
- [19] Yonggang Zhang, Xinmei Tian, Ya Li, Xinchao Wang, and Dacheng Tao, "Principal component adversarial example," in *IEEE Transactions on Image Processing*, 2020, vol. 29, pp. 4804-4815.
- [20] Jianyu Wang, and Haichao Zhang, "Bilateral adversarial training: Towards fast training of more robust models against adversarial attacks," in *Proceedings of the IEEE/CVF International Conference on Computer Vision (ICCV)*, 2019, pp. 6629-6638.
- [21] Dinghuai Zhang, Tianyuan Zhang, Yiping Lu, Zhanxing Zhu, and Bin Dong, "You only propagate once: Painless adversarial training using maximal principle," in *33rd Conference on Neural Information Processing Systems(NIPS)*, 2019.
- [22] Lawrence Cayton, "Algorithms for manifold learning," Univ. Ca San Diego, San Diego, CA, USA, Tech. Rep. CS2008-0923, 2005, vol. 12, pp. 1–17.
- [23] P.-A. Absil, R. Mahony, and R. Sepulchre, "Optimization Algorithms on Matrix Manifolds," Princeton University Press, Princeton, 2008.
- [24] Leslie N Smith, "Cyclical learning rates for training neural networks," in *2017 IEEE Winter Conference on Applications of Computer Vision (WACV)*, 2017, pp. 464–472.
- [25] Leslie N Smith and Nicholay Topin, "Super-convergence: Very fast training of residual networks using large learning rates," in *Artificial Intelligence and Machine Learning for Multi-Domain Operations Applications*, 2019.